The breakthrough curve combination for xenon sampling dynamic in a carbon molecular sieve column

Liu Shu-jiang[*], Chen Zhan-ying, Chang Yin-zhong, Wang Shi-lian, Li Qi, Fan Yuan-qing, Jia Huai-mao, Zhang Xin-jun, Zhao Yun-gang

CTBT Beijing National Data Centre and Radionuclide Laboratory, Beijing 100085, China

ABSTRACT: In the research of xenon sampling and xenon measurement, the xenon breakthrough curve plays a significant role in the xenon concentrating dynamics. In order to improve the theoretical comprehension of xenon concentrating procedure from the atmosphere, method on the breakthrough curve combination for sampling techniques should be developed and investigated for pulse injection condition. In this paper, we describe xenon breakthrough curve in a carbon molecular sieve column, the combination curves method for five conditions are shown and debated in detail; the fitting curves and the prediction equation are derived in theory and verified by the designed experiments. As a consequence, the curves of the derived equation are well agreement with the fitting curves by tested. The retention time of the xenon in the column are 61.2, 42.2 and 23.5 at the flow rate of 1200, 1600 and 2000 mL/min respectively, but the breakthrough time are 51.4, 38.6 and 35.1 min.

Keywords: curve combination, sampling dynamic, carbon molecular sieve, packed column.

1 Introduction

The compound breakthrough curve combinations, which include the adsorption and desorption, are important for theoretical prediction of the dynamics behavior on its separation and preparation technology. In order to demonstrate the dynamic behavior of the compound's adsorption, the ideal adsorbed solution theory (IAST) was developed under several assumptions for binary system, and four types of the adsorption isotherm was shown in much research [1, 2]. Similarly, some researchers used the IAST and Monte Carlo simulation methods to evaluate the design of Metal−Organic Framework Material [2, 3]. Using IAST calculation, the adsorption capacity of one component was also predicted precisely and the components selectivity was obtained under ideal conditions [4, 5]. As an alternative to the adsorption measurement, the breakthrough curve fitting was an indispensable method to evaluate one component adsorption capacity within two or more compounds [6, 7]. Furthermore, the breakthrough experiment was an effective tool to compare the material adsorption performances for practical sampling application [8~11].

Xenon, one of the noble gases, is a valuable commodity for its comprehensive applications in optics, illumination, medical science and nuclear technology [10~13]. As of 1996, the comprehensive nuclear-test-ban treaty (CTBT) was adopted for decades and xenon was also extendedly regarded as excellent "fingerprint" isotopes to monitor the nuclear test affairs [8, 10,14]. In order to improve the xenon monitoring level, some technologies on xenon sampling and xenon measurement were applied and developed, and gas chromatography was a classical method which was used to obtain xenon from ambient atmosphere [9]. While tremendous effort has been made on xenon sampling, transferring and purification over the last several decades, it remains some challenge to enrich xenon from ambient atmosphere, especially for the dynamics or mechanics of the xenon sampling [6~7, 15]. Xenon sampling was influenced by the efficiency of the sample injecting, transferring and separating, all of these factors were determined by the dynamics of the xenon sampling. During the complicated procedures of xenon sampling, much re-

* Corresponding author. Tel.: +86 013521330936.
E-mail addresses: liushu116@163.com, shujiang.liu@nrl.org.cn

search have been expended to understand the dynamics, and the dynamics of some ideal conditions, the multi-pulse injection and the injection volume, were also studied in detail [16~18]. At the same time, to improve the separation efficiency some new chromatography related technologies were designed [19~22] and the methods on technologies combinations such as multi-dimensional chromatography were also developed. Therefore, the components separation dynamics in a chromatograph were still very necessary before improving the column efficiency [23].

In this study, the curve combination equations are derived on the basis of the exponential modified gaussian (EMG) equation and the Boltzman equation. In order to verify these equations, the experimental apparatus is set up and the combination method is developed to derive the curves functions for five possible combination conditions.

2 Experimental apparatus and procedure

2.1 Experimental apparatus

The Experimental apparatus is made up of a gas supplier, a pulse injector, the packed column within carbon molecular sieve (CMS), two sampling valve fixed in the front and back of the packed column, the temperature control unit and its accessories, as shown in Fig. 1. The Fans gas supplier is a xenon pre-concentrating unit with a membrane, a cool dryer and a gas compressor, the gas out of the Fans gas supplier mainly contains nitrogen, and enriched noble gases such as argon, krypton and xenon. The pulse injector consists of the stainless steel tube and two quick coupling couplers, and its dead volume is 14.4mL. The CMS packed column is a stainless tube within 20 mesh CMS particulate which is made from Shan-Li chemical material Co. Ltd. During the whole experiment, the column temperature was controlled at 25 °C and the gas pressure was 8 atm.

Fig.1. Schematic illustration of the packed column within CMS for a curve combination.

2.2 Experimental procedure

In Fig. 1, the gas mixture from the Fans gas supplier is transferred into the CMS column, xenon inference gas (30% v/v with nitrogen as diluted gas, Beijing HaiPu Gas Development) in the pulse injector is prepared before being carried into the experimental apparatus by the gas mixture and gas valves controlled. The measured samples are obtained by the sampling valves set at the front and the back of the column. Although there are the other methods for xenon detection[24], the xenon concentrations are measured by the GCMS (Agilent Technology Ltd., USA) in this paper. GC−MS is done on an Agilent 7890 GC interfaced to a 5975C MS detector and containing a Restek 30 m × 0.32 mm i.d. capillary column (5Å molecular sieve, 0.25 μm film thickness). After pulsed split injection (1:20) of this mixture (5 mL) at 110 °C, the oven temperature is controlled at 100 °C. The helium carrier gas is maintained at a constant flow of 1 mL/min. Electron-impact MS data are tested in selected-ion-detected mode (m/z: 129, 130, 131, 132,134, 136) and analyze with Agilent Chemstation software.

The experimental procedure is designed as followed: the xenon breakthrough curves are discussed for two different conditions, pulse injection and typical adsorption. And then the curves' combination principal is proposed and derived under several assumptions. At last, the experimental verification is done and the combination curves are fitted and derived reasonably.

3 Results and discussion

3.1 The performances of the Boltzman and the Exponential Modified Gaussian equations

The Boltzman equation can be expressed in the form such as formula (1), the variable y is the xenon concentration flew out of the column, x means the time after injecting in the column.

$$y = A_2 + \frac{A_1 - A_2}{1 + e^{\frac{x - x_1}{dx}}} \tag{1}$$

Where both A_1 and A_2 are quantified in the breakthrough experiment, A_1 is determined by the xenon adsorption efficiency in the column, and usually nearly equivalent to the zero[6, 7]; A_2 is determined by the xenon concentration before injection; x_1 is defined as the half breakthrough time, as shown in Fig. 2(a).

The performances of the EMG equation is expressed in the form such as formula (2), in this equation variable y is also the xenon concentration flew out of the column, and x means the time after injecting in the column.

$$y = D_1 + \frac{D_2}{D_3 \sqrt{\pi / 2}} e^{\frac{-2(x - x_2)^2}{D_3^2}} \tag{2}$$

Where, all of the D_1, D_2 and D_3 are quantified in the breakthrough experiment, their definitions and relationships are discussed and derived in the references [18], x_2 is defined as the retention time, and the typical curve of the EMG equation was also shown in Fig. 2(b). In the xenon breakthrough experiment, D_1 is determined by the xenon adsorption efficiency in the column and equaled to the baseline value of a peak, and usually nearly equivalent to the zero, D_2 is used to calculate the width of a chromatographic peak, D_2 and D_3 are used to calculate the height of a chromatographic peak.

Fig.2. The typical graphics and physical performances of both the Boltzman and the EMG equations.

3.2 The xenon curves for the pulse injection and the breakthrough

As the former depiction, it is assumed that the combined equation can be derived as equation (3),

$$y = k(1) + (2) = (kA_2 + D_1) + k\frac{A_1 - A_2}{1 + e^{\frac{t - x_1}{dx}}} + \frac{D_2}{D_3 \sqrt{\pi / 2}} e^{\frac{-2(t - x_2)^2}{D_3^2}} \tag{3}$$

Where k is the combination ratio of the Boltzman equation, and there is y equals C as the x equals positive infinite, and there will be five kinds of combination curves, as shown in Fig.3. Firstly, we can consider the extreme conditions, if the k is big enough and the combination equation is mainly determined by the equation (1), and the combined curve can be depicted as Fig.3(a), another the k is very small and the combination equation is mainly determined by the equation (2), and the combined curve can be depicted as Fig.3 (b). When k equals a suitable value under non extreme condition, the combination equation is determined by both equation (1)and (2), and the curves for x_1 bigger or smaller than x_2, or equivalent to x_2 are shown in Fig.3 (c)~(e), respectively. As equation (3) definition, k can be transferred into the form as equation (4):

$$k = \frac{C - D_1}{A_2} \tag{4}$$

On the other hand, if the data can be measured and obtained in certain way, how to calculate the factor k is a key point to fit the curve function. Obviously, the curves in Fig.3(a) and (b) are fitted as the Boltzman and the EMG functions individually; the combined curves fitting in Fig.3(c) and (d) can be divided into two steps, the value of the factor k is assumed to equal one firstly, then the values of x_1 and x_2 can be calculated by the graph, the Boltzman and the EMG functions can be used to fit curve under different range of the time. But under the fifth condition, the combined curve is influenced by these two functions under the same time period, as shown in Fig.3(e).

Fig.3. The typical graphics for the combinations of between the Boltzman and the EMG equations.

3.3 The xenon curves for the pulse injection and the breakthrough

When the xenon injection volume is 0mL, the flow rate are 1200mL/min, 1600 mL/min and 2000mL/min, the xenon curves flowed out of the column are measured and fitted in Fig.4(a), (b) and (c), respectively; the formulas are also subsequently expressed as formula (5), formula (6) and formula (7):

Fig.4. The outflow curve for 0 mL xenon injection with the flow rate of: (a) 1200 mL/min. (b) 1600 mL/min. (c) 2000 mL/min.

$$y = 196 + \frac{0.40 - 196}{1 + e^{\frac{t - 61.2}{7.88}}} \tag{5}$$

$$y = 176 + \frac{-1.29 - 176}{1 + e^{(\frac{t - 42.2}{6.45})}} \tag{6}$$

$$y = 266 + \frac{-5.98 - 266}{1 + e^{(\frac{t - 23.5}{6.75})}} \tag{7}$$

Where t is the time of xenon injection, min. Under the flow rate of 1200 mL/min we obtain that A_1 equals 0.40, A_2 equals 196, and x_1 equals 61.2. According to formula (6) A_1 equals -1.29, A_2 equals 176, and x_1 equals 42.2 with the flow rate of 1600 mL/min. By formula (7), A_1 equals -5.98, A_2 equals 266, and x_1 equals 23.5 with the flow rate of 2000 mL/min.

When the xenon injection volume is 4.4 mL and the flow rate is 1200mL/min, the breakthrough curve is tested and fitted in Fig.5. According to Fig.5, the curve obeys exponential modified Gaussian distribution and its formula is expressed in formula (8).

Fig.5. The outflow curve for 4.4mL xenon injection with the flow rate of 1200 mL/min.

$$y = 829 + \frac{8.51 \times 10^6}{29.4\sqrt{\pi/2}} e^{\frac{-2(t-51.4)^2}{29.4^2}} \tag{8}$$

According to formula (8), we obtain that D_1 equals 829, D_2 equals 8.51×10^6, and D_3 equals 29.4.

When the xenon injection volume is 2.03 mL and the flow rate is 1600mL/min, the breakthrough curve is fitted in black points and line in Fig.6, and C equals 162 and the k is equal to 0.92, and the curve of k by equation (6) is shown in red points and line, and the tested data minus the results of the k by equation (6) at the same time is shown in blue and the curve is fitted by EMG distribution, the derived curve formula is expressed in equation (9).

Fig.6. The curves comparison between the tested and the fitted for 2.03mL xenon with 1600 mL/min.

$$y = 7.24 + \frac{5427}{28.2\sqrt{\pi/2}} e^{\frac{-2(t-48.6)^2}{28.2^2}} \tag{9}$$

According to equation (9), the k is equal to 0.88. Therefore, the combined equation is derived in equation (10) and its curve is depicted in green line in Fig.6.

$$y = 7.24 + \frac{5427}{28.2\sqrt{\pi/2}} e^{\frac{-2(t-48.6)^2}{28.2^2}} + \frac{162-7.24}{176}(176 + \frac{-1.29-176}{1+e^{(\frac{t-42.2}{6.45})}}) \tag{10}$$

When the xenon injection volume is 0.88 mL and the flow rate is 2000mL/min, the xenon concentration flowed out of the column is tested and the breakthrough curve is fitted in black points and line in Fig.7, and C equals 200 and the k is equal to 0.75, and the curve of k by equation (7) is shown in red points and line, and the tested data minus the results of the k by equation (7) at the same time is shown in blue and the curve is fitted by EMG distribution, the derived curve formula is expressed in equation (11).

Fig.7. The curves comparison between the tested and the fitted for 0.88mL xenon with 2000 mL/min.

$$y = 3.14 + \frac{8294}{18.8\sqrt{\pi/2}} e^{\frac{-2(t-35.1)^2}{18.8^2}} \tag{11}$$

According to equation (11), the k is equal to 0.74. Therefore, the combined equation can be derived in equation (12) and its curve is depicted in green line in Fig.7.

$$y = 3.14 + \frac{8294}{18.8\sqrt{\pi/2}} e^{\frac{-2(t-35.1)^2}{18.8^2}} + \frac{(200-3.14)}{266}(266 + \frac{-5.98-266}{1+e^{(\frac{t-23.5}{6.75})}}) \tag{12}$$

The verifications of formulas (10) and (12) are done in Fig.8(a) and (b), the derived curve is also drawn in green line, the tested curve is fitted in black points and line, the fitting curves by the EMG equation and the Boltzman equation are shown in red line and blue line. The Fig.8 illustrates that the derived curves are better agreement with the fitting curves by tested than the fitting curves only by the EMG equation or the Boltzman equation.

Fig.8. The derived combination curves verification for 1600 mL/min and 2000 mL/min.

Make comparisons between the formulas (5) and (8), (6) and (9), (7) and (11), we obtain the values of the half breakthrough time x_1 and the retention time x_2, as shown in Table 1. In contrast, at the flow rate of 1200 mL/min the half breakthrough time is bigger than the retention time, but samller than the retention time at the flow rate of 1600 mL/min and 2000 mL/min.

Table1 the half breakthrough time and the retention time under different flow rate.

| Flow rate/(mL/min)	x_1/min	x_2/min	remark
1200	61.2	51.4	$x_{01}>x_{02}$
1600	42.2	48.6	$x_{01}<x_{02}$
2000	23.5	35.1	$x_{01}<x_{02}$

4 Conclusion

In summary, we fit, examine and discuss the xenon combination curves for five given conditions of a pulsed injecting and a breakthrough, these five curves fitting methods are developed and their equations are derived under the given assumption. As a consequence, the fitting equation of the xenon breakthrough curve could be regarded as the combination of the breakthrough equation and the outflow equation under the experimental conditions. These investigations also demonstrate that the relationship be-

tween the half breakthrough time and the retention time is influenced by the flow rate in the CMS column.

References

[1] M. Mazzotti, A. Tarafder, A method for deriving explicit binary isotherms obeying the ideal adsorbed solution theory. Chem. Eng. Technol. 35(1) (**2012**) 102.

[2] S. T. Meek, S. L. Teich-McGoldrick, J. J. Perry IV, J. A. Greathouse, M. D. Allendorf, Effects of polarizability on the adsorption of noble gases at low pressures in monohalogenated isoreticular Metal−Organic Frameworks. J. Phys. Chem. C 116(**2012**) 19765.

[3] F. C. Naomi, A. S. Nigel, D. Tina, Evaluation of ideal adsorbed solution theory as a tool for the design of Metal−Organic Framework materials. Ind. Eng. Chem. Res. 51(**2012**) 4911.

[4] H. Wang, K.X. Yao, Z.J. Zhang, J. Jagiello, Q.H. Gong, Y. Han, J. Li, The first example of commensurate adsorption of atomic gas in a MOF and effective separation of xenon from other noble gases. Chem. Sci. 5(**2014**) 620.

[5] Z. Hulvey, K. V. Lawler, Z.W. Qiao, J. Zhou, D. Fairen-Jimenez, R. Q. Snurr, S. V. Ushakov, A. Navrotsky, C. M. Brown, P. M. Forster, Noble gas adsorption in copper trimesate, HKUST-1: an experimental and computational study. J. Phys. Chem. C 117(**2013**) 20116.

[6] C.Y. Zhou, S.J. Feng, G.Q. Zhou, Y.R. Jin, J.F. Liang, J.M. Xu, the behavior of xenon dynamic adsorption on granular activated carbon packed bed adsorber. J. Radioanal. Nucl. Chem 287(**2011**) 609.

[7] C.Y. Zhou, Y.R. Jin, H. Xu, S.J. Feng, G.Q. Zhou, J.F. Liang, J.M. Xu, Use of Wheeler–Jonas equation to explain xenon dynamic adsorption breakthrough curve on granular activated carbon. J. Radioanal. Nucl. Chem 288(**2011**) 251.

[8] S.L. Wang, Q. LI, Q.H. Meng, Z.Y. Chen, Y.G. Zhao, H.J. Li, H.M. Jia, Y.Z. Chang, S.J. Liu, X.J. Zhang, Y.Q. Fan, L. Wan, Y. Lou, Radio xenon monitoring in Beijing following the Fukushima Daiichi NPP accident. Appl. Radiat. Isot. 81(**2013**) 344.

[9] L. Tuula, ¨O. Conny, C. Anders, An automated multidimensional preparative gas chromatographic system for isolation and enrichment of trace amounts of xenon from ambient air. Anal. Bioanal. Chem 400(**2011**) 449.

[10] J. Liu, P. K. Thallapally, D. Strachan, Metal−Organic Frameworks for removal of Xe and Kr from nuclear fuel reprocessing plants. Langmuir 28(**2012**) 11584.

[11] M. Taguchi, I. Yagi, M. Nakagawa, T. Iyoda, Y. Einaga, Photocontrolled magnetization of CdS-modified prussian blue nanoparticles. J. Am. Chem. Soc. 128(**2006**) 10978.

[12] J. F. Lehmann, H. P. A. Mercier, G. J. Schrobilgen, The chemistry of krypton. Coord. Chem. Rev. 233-234(**2002**) 1.

[13] M. Fernandez-Alvarez, M. Lores, E. Jover, C. Garcia-Jares, J. M. Bayona, M. Llompart, Photo-solid-phase microextraction of selected indoor air pollutants from office buildings. Identification of their photolysis intermediates. J. Chromatogr. A 1216(**2009**) 8969.

[14] J.P. Fontaine, F. Pointurier, X. Blanchard, T. Taffary, Atmospheric xenon radioactive isotope monitoring. J Environ. Radioact. 72(**2004**) 129.

[15] C. A. Fernandez, J. Liu, P. K. Thallapally, D. M. Strachan, Switching Kr/Xe selectivity with temperature in a Metal−Organic Framework. J. Am. Chem. Soc. 134(**2012**) 9046.

[16] S. J. Liu, Z. Y. Chen, S. L. Wang, Y. Z.Chang, Q. Li, Y. Q. Fan, Y. G. Zhao, H. M. Jia, X. J. Zhang, J. Wang, Fitting formula for the injection volume of a gas chromatograph for radio-xenon sampling in the lower troposphere, J. Sep. Sci. 37(2014) 1456.

[17] S. J. Liu, Z. Y. Chen, Y. Z. Chang, S. L. Wang, Q. Li, S. J. Fang, Y. Q. Fan, Y. G. Zhao, Resolutions on mixture of argon, krypton, xenon and radon by gas chromatograph, At. Energy Sci. Technol. 46(2012)27.

[18] S. J. Liu, Z. Y. Chen, Y. Z.Chang, S. L. Wang, Q. Li, Y. Q. Fan, Inference and analysis of xenon outflow curves under multi-pulse injection in two-dimensional chromatography. J. Chromatogr. A 1311(**2013**) 183.

[19] A. Pukalskas, T. A. V. Beek, P. D. Waard, Development of a triple hyphenated HPLC–radical scavenging detection–DAD–SPE–NMR system for the rapid identification of antioxidants in complex plant extracts. J. Chromatogr. A 1074(**2005**) 81.

[20] A. Avalli, G. Contarini, Determination of phospholipids in dairy products by SPE/HPLC/ELSD. J. Chromatogr. A 1071(**2005**) 185.

[21] H. R. Lee, S. M. Cho, J. Kim, D. S. Chung, Novel and simple headspace in-tube microextraction coupled with capillary electrophoresis. J. Chromatogr. A 1346(**2014**) 117.

[22] R.L. Hu, Y.J. Pan, Recent trends in counter-current Chromatography. TrAC. Trends Anal. Chem. 40(**2012**) 15.

[23] P. J. Marriott, S. T. Chin, B. Maikhunthod, H. G. Schmarr, S. Bieri, Multidimensional gas Chromatography. Trends Anal. Chem. 34(**2012**) 1.

[24] O. Hayden, U. Latif, and F. L. Dickert, A Mass-Sensitive Approach for the Detection of Anaesthetic Xenon, Aust. J. Chem., 64(2011) 1628.
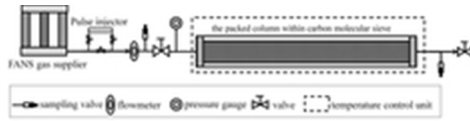
19x4mm (300 x 300 DPI)
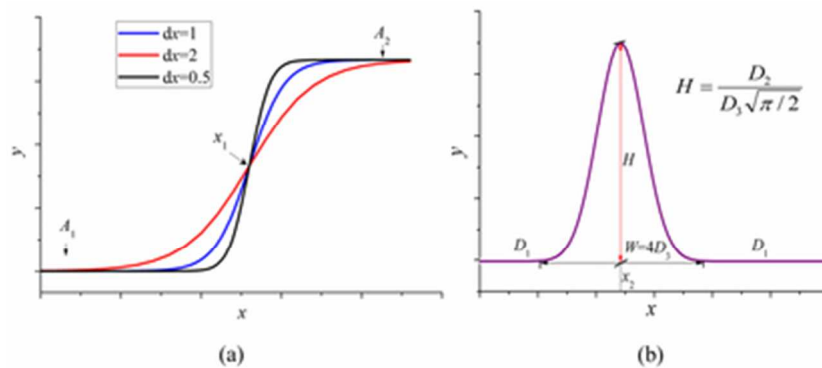
35x15mm (300 x 300 DPI)
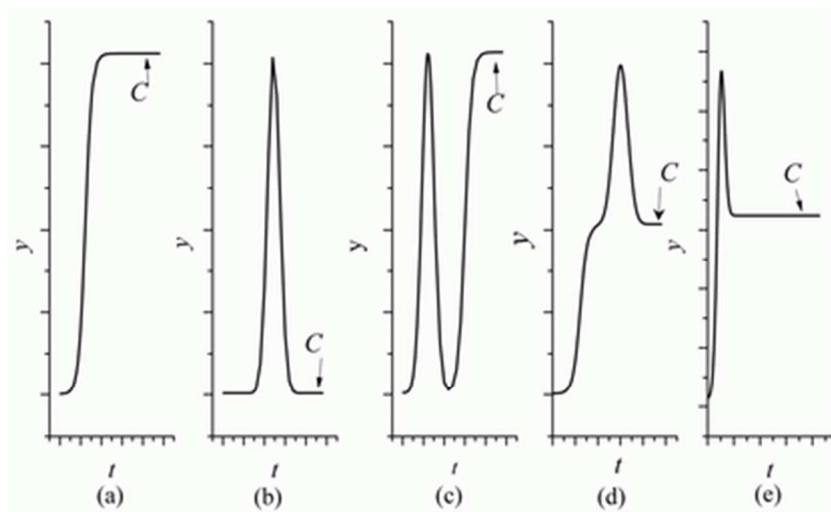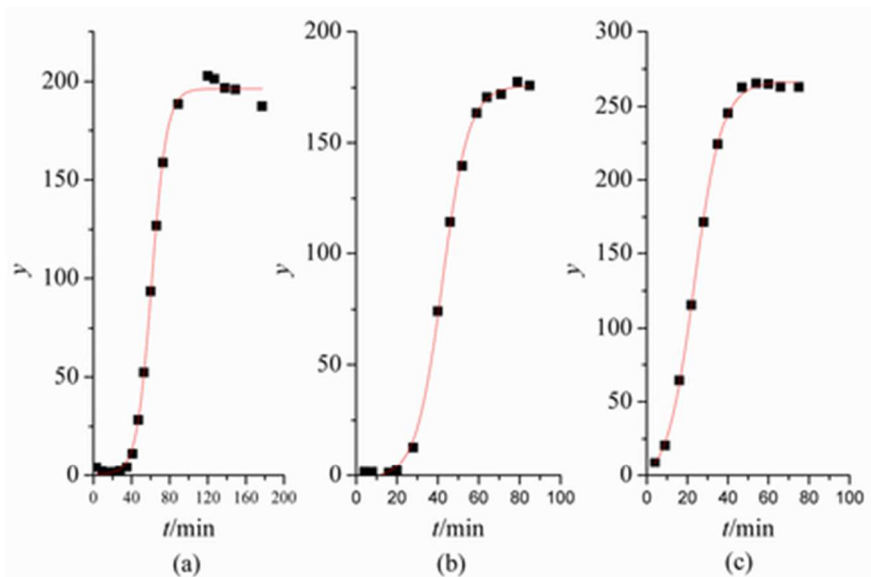
35x21mm (300 x 300 DPI)

36x24mm (300 x 300 DPI)
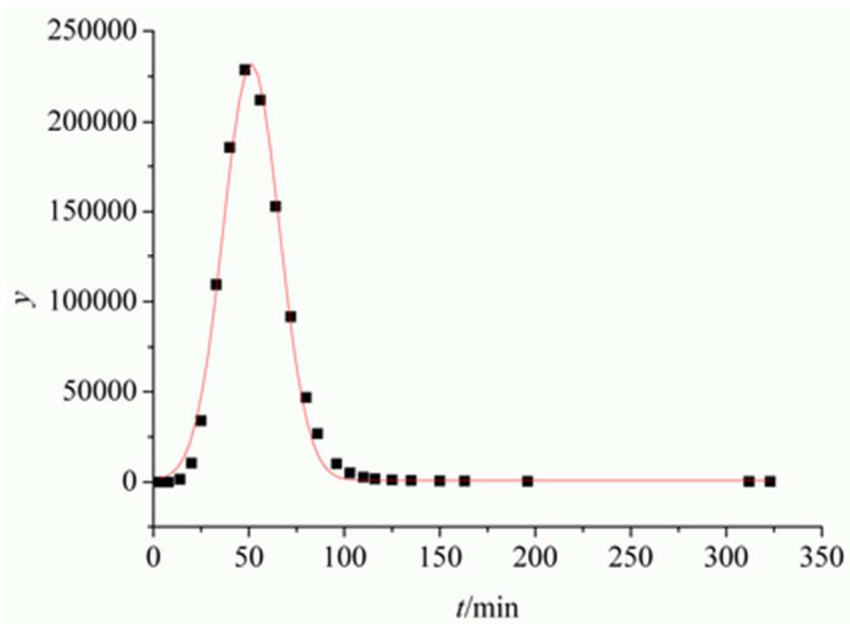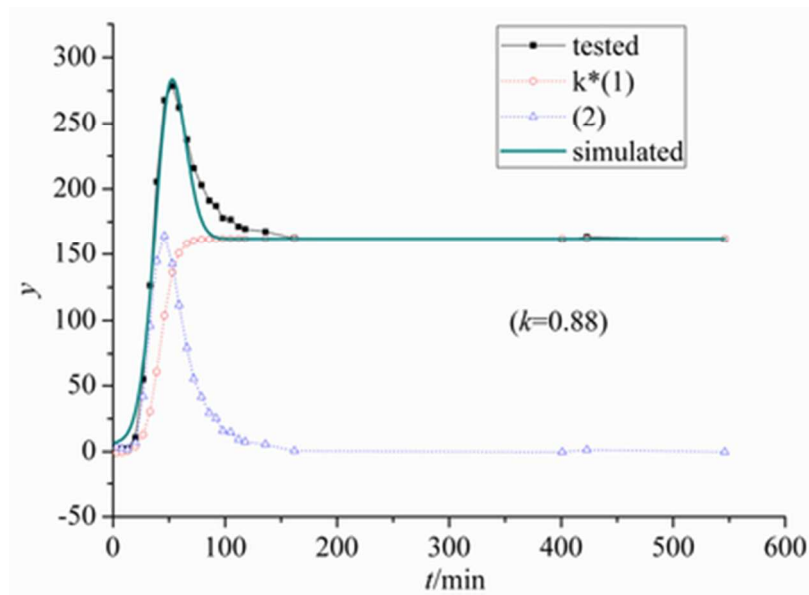
35x26mm (300 x 300 DPI)

34x24mm (300 x 300 DPI)
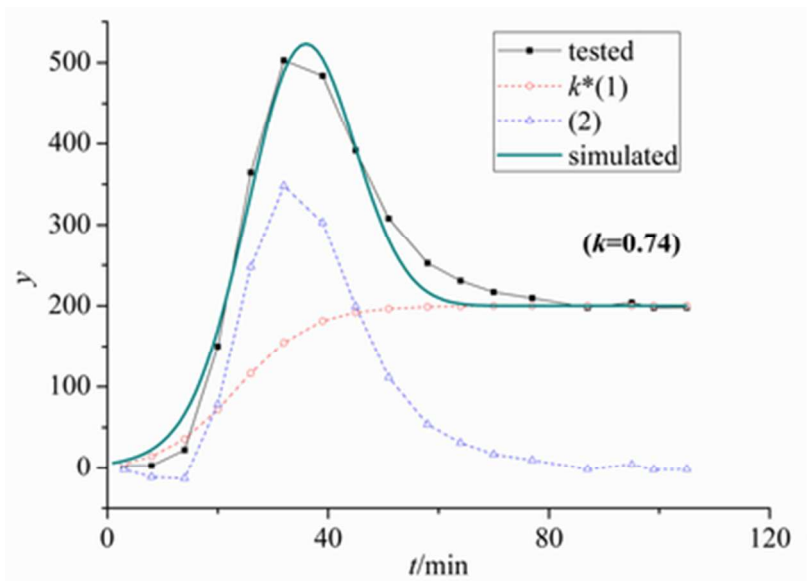
33x24mm (300 x 300 DPI)

39x16mm (300 x 300 DPI)